A Risk-Based Approach for Aerothermal/ TPS Analysis and Testing

Michael J. Wright* **and Jay H. Grinstead†**
NASA Ames Research Center, MS 230-2
Moffett Field, CA 94035
USA

Deepak Bose‡
ELORET Corp.
Sunnyvale, CA 94089
USA

ABSTRACT

The current status of aerothermal and thermal protection system modeling for civilian entry missions is reviewed. For most such missions, the accuracy of our simulations is limited not by the tools and processes currently employed, but rather by reducible deficiencies in the underlying physical models. Improving the accuracy of and reducing the uncertainties in these models will enable a greater understanding of the system level impacts of a particular thermal protection system and of the system operation and risk over the operational life of the system. A strategic plan will be laid out by which key modeling deficiencies can be identified via mission-specific gap analysis. Once these gaps have been identified, the driving component uncertainties are determined via sensitivity analyses. A Monte-Carlo based methodology is presented for physics-based probabilistic uncertainty analysis of aerothermodynamics and thermal protection system material response modeling. These data are then used to advocate for and plan focused testing aimed at reducing key uncertainties. The results of these tests are used to validate or modify existing physical models. Concurrently, a testing methodology is outlined for thermal protection materials. The proposed approach is based on using the results of uncertainty/sensitivity analyses discussed above to tailor ground testing so as to best identify and quantify system performance and risk drivers. A key component of this testing is understanding the relationship between the test and flight environments. No existing ground test facility can simultaneously replicate all aspects of the flight environment, and therefore good models for traceability to flight are critical to ensure a low risk, high reliability thermal protection system design. Finally, the role of flight testing in the overall thermal protection system development strategy is discussed.

1.0 INTRODUCTION

Any Earth or planetary entry vehicle will be subjected to significant aerothermal heating as it dissipates its kinetic energy at the destination planet (or moon). The primary purpose of the thermal protection system (TPS) is to protect the payload (crew, cargo, or science) from this entry heating environment. The performance of the TPS is determined by the efficiency and reliability of this system, typically measured

* Senior Research Scientist, Reacting Flow Environments Branch. e-mail address: Michael.J.Wright@nasa.gov

† Senior Research Scientist, Reacting Flow Environments Branch. e-mail address: Jay.H.Grinstead@nasa.gov

‡ Senior Research Scientist. e-mail address: dbose@ionamerica.com

Wright, M.J.; Grinstead, J.H.; Bose, D. (2007) A Risk-Based Approach for Aerothermal/TPS Analysis and Testing. In *Experiment, Modeling and Simulation of Gas-Surface Interactions for Reactive Flows in Hypersonic Flights* (pp. 17-1 – 17-24). Educational Notes RTO-EN-AVT-142, Paper 17. Neuilly-sur-Seine, France: RTO. Available from: http://www.rto.nato.int/abstracts.asp.

Report Documentation Page

Form Approved
OMB No. 0704-0188

1. REPORT DATE	2. REPORT TYPE	3. DATES COVERED
01 JUL 2007	**N/A**	**-**

4. TITLE AND SUBTITLE	5a. CONTRACT NUMBER
A Risk-Based Approach for Aerothermal/TPS Analysis and Testing	5b. GRANT NUMBER
	5c. PROGRAM ELEMENT NUMBER
6. AUTHOR(S)	5d. PROJECT NUMBER
	5e. TASK NUMBER
	5f. WORK UNIT NUMBER
7. PERFORMING ORGANIZATION NAME(S) AND ADDRESS(ES) **NASA Ames Research Center, MS 230-2 Moffett Field, CA 94035 USA**	8. PERFORMING ORGANIZATION REPORT NUMBER
9. SPONSORING/MONITORING AGENCY NAME(S) AND ADDRESS(ES)	10. SPONSOR/MONITOR'S ACRONYM(S)
	11. SPONSOR/MONITOR'S REPORT NUMBER(S)

12. DISTRIBUTION/AVAILABILITY STATEMENT
Approved for public release, distribution unlimited

13. SUPPLEMENTARY NOTES
See also ADM002058., The original document contains color images.

14. ABSTRACT

15. SUBJECT TERMS

16. SECURITY CLASSIFICATION OF:			17. LIMITATION OF ABSTRACT	18. NUMBER OF PAGES	19a. NAME OF RESPONSIBLE PERSON
a. REPORT	b. ABSTRACT	c. THIS PAGE			
unclassified	**unclassified**	**unclassified**	**UU**	**24**	

Standard Form 298 (Rev. 8-98)
Prescribed by ANSI Std Z39-18

in terms of the total mass of material and associated sub-structure required to protect the payload to a prescribed level of risk-tolerance. Therefore, for a rigid or flexible aeroshell, the choice and design thickness of the TPS material are key performance metrics. The choice of the TPS material is typically governed by the peak heat flux, surface pressure, and shear stress encountered during the entry, with more robust (higher density) materials required to protect the vehicle from more severe entry conditions. The thickness of the chosen material is governed by the total integrated heat load during the entry (which can be very large for aerocapture or lifting-body cruise missions, due to a long residence time in the atmosphere [1]). The determination of these quantities relies on aerothermodynamics and material response modeling as well as ground-based testing in flight-relevant environments to ensure adequate material performance.

For most missions of interest, no ground test can simultaneously reproduce all aspects of the flight environment. Therefore, a good understanding of the relevant physics is required to trace ground testing results to predicted flight performance metrics. The design and operation of reliable TPS requires accurate knowledge of the incident environment and resulting material response. Our ability to accurately and conservatively simulate the environment and the material response directly affects TPS risk, mass and reliability. Improving the accuracy of the underlying physical models will enable a greater understanding of the system-level impacts of a particular thermal protection system and of the system operation and risk over its operational life. Prior experience with both reusable and ablative TPS is that the accuracy of our simulations is typically limited not by the tools and processes currently employed, but rather by reducible deficiencies in the underlying physical models. Fortunately, while specific modeling deficiencies are very mission dependent, in general they can be divided into several broad categories: nonequilibrium gas kinetics, shock-layer radiation, transition and turbulent heating, afterbody heating, gas-surface interactions, and coupling between the TPS material and the flow environment.

Although baseline predictions of the aerothermal environment and resulting material response are made using high-fidelity modeling and simulation tools, the evaluation of associated uncertainties often involves comparatively little or no rigor. However, an accurate determination of these uncertainties is critical in ensuring selection of an appropriate material and in determining the resulting margin and factor of safety. An accurate assessment of TPS risk is required to ensure that the sub-system design is consistent with the risk posture of the program. The results can also be incorporated with probabilistic design techniques [2][3] so that engineers can make informed decisions on ways to effectively balance mission risk between the TPS and other sub-systems. Historical approaches for dealing with these uncertainties have traditionally been somewhat ad-hoc, most commonly relying on expert judgment [4]. Even when rigorous attempts at uncertainty estimation were attempted [5][6], computational resource limitations prevented the sort of non-linear multivariate analysis that is truly required. Final “rolled-up” uncertainties are then typically determined using either a stacked worst-case approach, which can be needlessly conservative, or a root-sum-square approach, which is only appropriate for a set of small linearly independent errors. Worse yet, both of these approaches may in fact be non-conservative if the underlying component uncertainties are not estimated correctly [5]. This paper will briefly discuss a Monte-Carlo based methodology for physics-based probabilistic uncertainty analysis of aerothermodynamics and material response modeling, as detailed in Refs. [7] & [8]. A primary objective of this work is to quantify the uncertainties in vehicle heating and the resulting TPS sizing based on inaccuracies in the knowledge of the input parameters. In addition, the technique allows TPS designers to prioritize and target key input uncertainties for further testing [9] in order to maximize the return from limited research funding. The results of the analysis can also be used to assist in the identification of possible additional uncertainties due to erroneous or overly simplified physical models (also known as structural uncertainties); if the models employed are correct, the sensitivities predicted by the analysis should be reproducible via targeted experiments. Identification of structural uncertainties is a key element of this type of analysis, because a large undetected structural uncertainty can invalidate the design, resulting in a potentially non-conservative TPS solution.

Although high fidelity analysis is an essential element of TPS design, it is only one component of the overall program. The analysis tools employed are fundamentally supported by ground tests in high enthalpy test facilities that simulate the flight environment over a range of conditions and at appropriate time and length scales. Ground testing in these facilities is used to validate the simulation tools; develop and select TPS materials; and qualify the final material for flight [10]. For example, arc jet facilities have been a workhorse for TPS testing, design, and qualification in the United States for over 40 years. However, no single high enthalpy ground test facility can replicate all transatmospheric flight conditions for most missions of interest. Therefore, successful test planning strategies combine the advantages of different facilities with appropriate choices of test conditions to encompass, as thoroughly as possible, the critical features of the flight environment [11]. A validation effort is broken down into discrete components, with each component designed to stimulate a specific aerothermal or material response process through parametric variation of test conditions. The capabilities and shortcomings of the facilities employed must be understood when formulating test objectives, interpreting test results, and integrating the results across the ground test envelope. This paper outlines a testing strategy, first discussed by Grinstead et al. [10], intended to ensure that the testing performed is of maximum utility to the computational modeler and TPS designer. Pre- and post-test computational analysis, as well as non-intrusive experimental flowfield diagnostic techniques, play a critical role in ensuring ground to flight traceability of the resulting test data.

Finally, the role of flight testing in the overall TPS design and certification process must be explored. Flight testing, while certainly capable of fully exercising the TPS design, is prohibitively expensive in most cases. In general flight testing should be reserved for final model and system-level validation, once we have good physics-based models of the expected environment and resulting material performance. Ideally, the purpose of a dedicated flight experiment should not be to learn anything new about the flight environment encountered, but rather to validate that the models employed are adequate. While dedicated flight tests are rare, it should be noted that valuable engineering information could be obtained at a much lower cost by including engineering instrumentation on science missions. Such instrumentation has little benefit to the mission that flies it, but the overall exploration program benefits greatly from the additional knowledge gained about the flight environment, which can the be applied to improving the design of future missions.

2.0 IDENTIFICATION OF MODELING AND SIMULATION GAPS

Modeling gaps are deficiencies in the current state of the art that impair the fidelity of aeroheating or TPS sizing analysis. In general, civilian entry vehicles can be separated into three classes: reusable launch vehicles (RLV's), such as the Shuttle Orbiter, inflatable decelerators, such as ballutes, and entry capsules, such as all previous planetary probes, the Apollo Command Module, and the proposed NASA Crew Exploration Vehicle (CEV). Each of these vehicle classes has their own set of modeling gaps. For RLV analysis many of the primary gaps are in process improvement (e.g. grid generation over steps, gaps and control surfaces) [12][13]. The entry physics are generally well understood, although local effects around deflected control surfaces and gas-surface interactions (primarily catalysis) on the reusable TPS materials employed present significant challenges to the state of the art. Inflatable decelerator systems operate at a low ballistic coefficient, and are by definition flexible. Although such vehicles fly in a regime where heating rates are comparatively low, the materials employed have much lower performance limits than traditional rigid TPS materials [14], and thus are potentially more sensitive to large uncertainties. Principle modeling gaps for this class of entry systems include non-continuum and free molecular aeroheating as well as unsteady aeroelastic/aerothermal interactions [15]. Finally, capsules typically have much higher entry velocity than RLV's and can enter a variety of planetary atmospheres, each with unique thermochemistry. For this class of missions the accuracy of our simulations is typically limited not by the tools and processes currently employed, but rather by reducible deficiencies in the underlying physical models. These deficiencies, while very mission-specific, can be divided into several broad categories:

nonequilibrium gas kinetics, shock-layer radiation, transition and turbulent heating, afterbody heating, gas-surface interactions, and coupling between the TPS material and the flow environment.

In any case, the first step after identifying the key mission requirements is to perform a mission-specific gap analysis. In this process we first seek to determine knowns and "known-unknowns" via literature searches, analysis of existing ground test and flight data, and relevant previous mission studies. A baseline set of physical models is then selected that captures the important aspects of the entry environment. Sensitivity and uncertainty analyses are then used to quantify uncertainties in the physical models employed and prioritize the uncertainty drivers. This process is discussed in more detail in Section 3. However, it is important to note that such analyses, since they are looking only at the sensitivities in the physical models employed in the simulation, cannot be used in and of themselves to identify fundamental structural uncertainties, or "unknown-unknowns, in those models. These "unknown-unknowns" must be exposed through dedicated ground or flight testing. However, the objectives of this testing can be tailored by pre-test analysis, which can predict the trends and sensitivities that should be observed if the models employed are correct. This sequence of events allows for much greater focus of (presumably) limited testing resources, which can now be spent targeting only those uncertainties that are a) reducible and b) have a large impact on the performance of the overall TPS system.

2.1 Example: Mars Entry Convective Heating

In the current section, we examine key modeling gaps for Mars entry simulations. It is well known that the surface recombination of gas-phase atoms and radicals due to the catalytic activity of the wall is often a primary source of convective heating during Earth or planetary entry. However, the physical mechanism that governs the catalytic recombination process is poorly understood for non-Earth entries. In addition, the surface condition due to past history and exposure to other adsorbing species can alter the catalytic properties, making it further difficult to quantify and address flight traceability issues. Consequently, modeling of catalytic reactions at the surface has been relatively primitive, and constitutes a significant modeling gap for Mars entry simulations. In fact, for Mars entries the so-called supercatalytic wall model [16], in which the gas composition at the surface is specified to be equal to that in the freestream, is frequently employed as a design assumption [17], primarily because it is easy to implement in a CFD code, requires no knowledge of the actual surface processes, and provides a conservative upper bound to the predicted heating level.

In general, surface catalytic reaction models, such as the Langmuir-Hinshelwood (LH) or Eley-Rideal (ER) mechanisms, solve a surface site balance equation coupled with gas phase densities. In the LH model the recombining species are adsorbed on the surface prior to recombining, while in the ER mechanism a gas phase species recombines directly with an adsorbed species. Several prior simulations of Mars entry aeroheating have assumed an ER mechanism to describe wall catalysis because of its simplicity. For example, in the Mitcheltree and Gnoffo model [18], CO + O recombination is assumed to occur on the surface via a two-step ER process. However, the literature indicates that the LH mechanism is more commonly observed than the ER mechanism [19]. In fact, direct experimental evidence of ER mechanism under any condition is lacking.

While there have been some attempts to obtain experimental data and build corresponding theoretical models [20]–[24], none of these have yet described the surface chemistry of actual TPS materials at temperatures and conditions relevant to Mars entries. However, it is possible to bound the expected heat transfer rates by using a simplified flux-based model. We know that for moderate velocity Mars entry, the freestream CO_2 is almost completely dissociated into CO and O. Among the several possible surface recombination reactions, the following two have been proposed [18] [25] as the principal reactions that are likely to control surface catalytic heating:

$$CO + O \xrightarrow{\gamma_1} CO_2 \quad , \Delta E = 5.51 \text{ eV} \tag{1}$$

$$O + O \xrightarrow{\gamma_2} O_2 \quad , \Delta E = 5.16 \text{ eV} \tag{2}$$

The parameters γ_1 and γ_2 are the reaction probabilities for reactions (1) and (2) respectively. However, these parameters do not vary independently, since both reactions consume O-atoms. After some algebra [26], it is possible to recast reactions (1) and (2) in a form that accounts for both diffusion and rate limiting using two independent parameters: γ_{cat}, which controls the rate at which O-atoms are consumed at the surface via either reaction, and the preference factor, p_2, which determines the fraction of recombining O atoms that follow reaction (2) as opposed to (1). Each of γ_{cat} and p_2 can independently vary between 0 and 1. For γ_{cat}, a value of 0 corresponds to a non-catalytic wall, while a value of 1 corresponds to a fully catalytic wall at which all inbound O-atoms recombine via reactions (1) and (2). For p_2, a value of 0 indicates that all O-atoms that recombine do so via reaction (1), while a value of 1 indicates that reaction (2) is exclusively preferred. By varying these parameters, the entire window of catalycity can be spanned. For example, setting γ_{cat} = 0 results in a non-catalytic surface regardless of the value of p_2. The fully catalytic limit of the Mitcheltree model [18] can be reproduced by setting γ_{cat} = 1 and p_2 = 0. It should be noted that, to date, experimental studies on low temperature quartz and metallic surfaces [21][24], have shown no conclusive evidence of reaction (1), indicating that p_2 may in fact be quite large in flight applications.

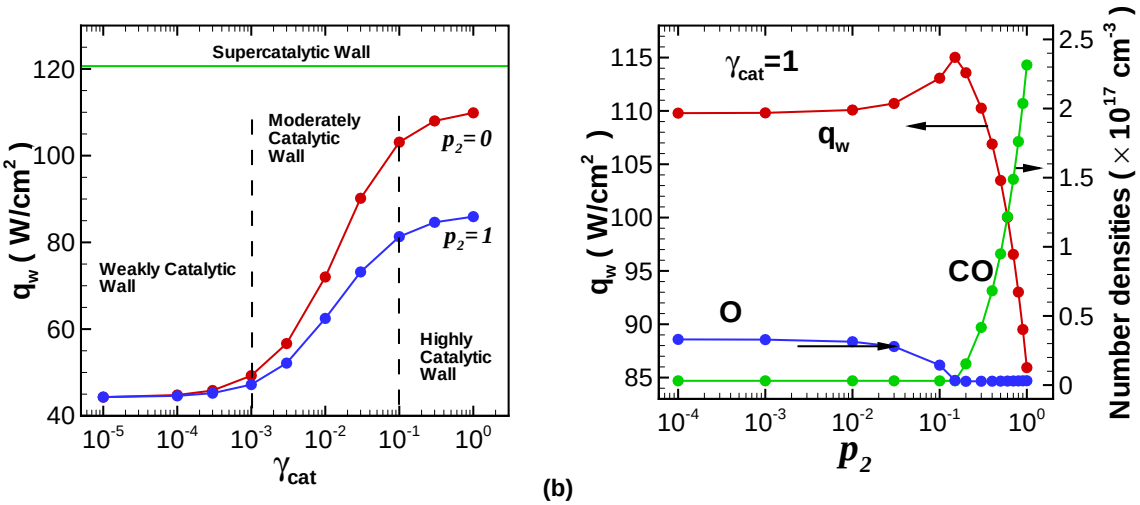

Figure 1 (a) Stagnation point heat flux variation for Mars Pathfinder with different levels of wall catalycity and preference factors and (b) variations of heat flux and wall number densities of gas phase CO and O with the preference parameter p_2, (γ_{cat} =1).

The drawback of this approach is that the parameters γ_{cat} and p_2 have unknown dependencies on factors like temperature, density, and surface condition. However, until sufficient experimental data are obtained to build a higher fidelity model, this approach is a useful tool to permit a systematic exploration of the parameter space and related sensitivities. For example, Fig. 1a shows the variation of the peak stagnation point heat flux (q_w) for Mars Pathfinder with γ_{cat} at the two extremes of the preference factor p_2. The curves in Fig. 1a have a distinctive "$\mathcal{S}$" shape that outline three distinct heating regimes as indicated by the vertical dashed lines. The first is the high catalytic efficiency region ($\gamma_{cat} > 0.1$), where the heat flux weakly varies with the value of γ_{cat} due to diffusion limiting. The second region in is the moderate catalytic efficiency regime ($10^{-3} < \gamma_{cat} < 10^{-1}$), where the heat flux is highly sensitive to γ_{cat} as the recombination rate is surface-process rate limited. The third region in Fig. 1a is the weakly catalytic regime ($\gamma_{cat} < 10^{-3}$), where the exact value of γ_{cat} is again unimportant to heating since wall catalycity contributes little to the total heat flux. Figure 1b shows the variation of the stagnation point heat flux and

the gas phase number densities of CO and O at the stagnation point versus the preference factor, p_2, assuming a fully catalytic wall (γ_{cat} =1). When p_2 is low, CO+O recombination is dominant, and both CO and O are efficiently utilized. Figure 1b shows that a slight excess of O atoms (caused by unequal diffusion rates) is seen. The extra O atoms can be further utilized if a small amount of O+O recombination is allowed to occur by raising p_2. This trend is evident in Fig. 1b as a drop in O density and a further rise of q_w as p_2 is increased. Once p_2 is raised above this critical value, the catalytic heating begins to sharply fall, because the stoichiometric requirement of the catalytic reactions no longer matches the available number density ratio of CO and O. As a result a rise in p_2 is accompanied by an under utilization of CO manifested as a rise in its density.

3.0 TYPES OF MODELING UNCERTAINTY

Over the years the nonequilibrium CFD and material response codes used for TPS sizing of entry vehicles have been calibrated against each other [27] and validated with a variety of experimental data from ground and flight tests [25], [28]–[31]. Based on these analyses, it can be clearly demonstrated that the predictions made by these tools are in most cases highly sensitive to the physical, chemical, and numerical models employed, as well as the multitude of input parameters that these models introduce [4]. As a result, the net uncertainty in heating and TPS sizing predictions is a result of a combined effect of the uncertainties in all of the models and input parameters used in the analysis. Therefore, in order to place confidence levels on an aeroheating or TPS sizing calculation, all of the chief sources of input uncertainty must be identified and quantified. The propagation of these uncertainties through the model must then be tracked to make probabilistic estimates of the resulting quantities, in the form of a most probable result and a probability distribution characterizing the variability of the prediction. The primary sources of uncertainty in the thermochemical models used in aerothermal and TPS analysis, like other physical models, can be classified into three categories: stochastic variability, parametric uncertainty, structural uncertainty. Each of these is discussed below:

1. Stochastic Variability. Arises due to natural fluctuations in the physical environment. Stochastic variability is also known as irreducible uncertainty, because it can be characterized, but not reduced, by analysis or testing. Examples in TPS design include fluctuations in atmospheric composition, temperature, or density, as well as small changes in entry flight path angle and vehicle orientation.

2. Parametric Uncertainty. Arises from the uncertainties in the input model parameter estimates. Parametric uncertainties can generally be reduced, but not eliminated, via focused testing or theoretical analysis. In an aerothermal CFD code, input variables include such things as kinetic reaction rates, vibration-dissociation coupling parameters, vibrational-translational relaxation times, binary interaction collision integrals for transport property calculations (diffusion, viscosity, and thermal conductivity coefficients), wall catalycity parameters, and possibly even freestream conditions. In a TPS material response code the input variables include virgin and char thermal conductivity, specific heats of the various components, surface emissivity, recession rate, initial cold soak temperature, and properties of the underlying sub-structure and overall material stack-up.

3. Structural Uncertainty. All numerical simulations employ mathematical models of the underlying physical processes. Structural uncertainties arise when the models employed, or their discretization, are incorrect or insufficient to adequately describe the phenomenon under study. Obviously, the potential for structural uncertainties in a given simulation is larger in regimes for which the models have not been properly validated. Examples of structural uncertainties include poor grid resolution or flux discretization scheme, using the Euler equations to simulate a viscous flowfield, or ignoring shock layer radiation for Apollo reentry simulations.

3.1 Example of a Structural Uncertainty: Radiative Heating at Titan

Saturn's largest moon Titan is a high priority target for future solar system exploration, with interest fueled in large part by the successful ESA Huygens probe entry in January 2005. Several ambitious follow-on surface missions have been proposed, including rovers and balloons. However, aeroheating predictions for both direct entry [32][33] and aerocapture [34] Titan entry missions to this point have indicated that a large portion of the total heat load during the entry could come from shock layer radiation. This radiative heating is due to the unique composition of the Titan atmosphere, which consists primarily of N_2 with a small amount (~2% by volume) of methane. This composition produces significant amounts of the CN radical behind the bow shock wave due to gas-phase chemical reactions. CN radiates strongly in the violet and red bands of the spectrum, even at fairly low entry velocities. Figure 2a shows predicted [35] convective and radiative heating levels to a typical Titan aerocapture vehicle with an entry velocity of 6.5 km/s. From the figure we see that the predicted radiative heating is nearly a factor of three higher than the convective heating on the aeroshell. In comparison, radiative heating rates at this entry velocity would be negligible for an Earth or Mars entry. Clearly these predicted heating rates, if real, will govern the TPS material selection and thickness for future Titan entry missions.

All of these analyses assumed that the radiative emission from the CN radical was governed by a Boltzmann (equilibrium) distribution of the low-lying excited states. While it was recognized [34] that this simple model was not validated for Titan entries, it was selected because there were no applicable ground test or flight data with which to develop a better model, and it was deemed likely (but not certain) that the Boltzmann assumption would provide a conservative estimate of the resulting radiative heat flux. The assumption of a Boltzmann distribution thus constituted a potentially large structural uncertainty for this analysis.

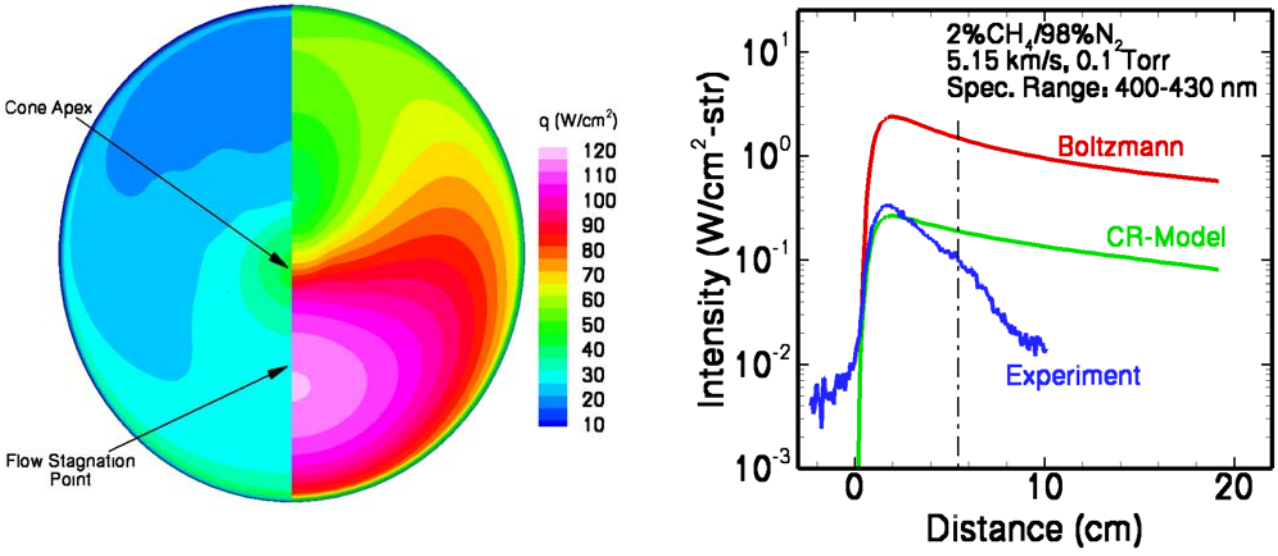

Figure 2 a) comparison of convective (left) and radiative (right) heating rates on a potential Titan aerocapture vehicle, and b) comparison of the Boltzmann and Collisional-Radiative (CR) models to experimental data for Titan shock layer radiation.

In order to address this concern, shock tube data were obtained recently in the Electric Arc Shock Tube (EAST) facility at NASA Ames and analyzed to measure radiation behind shock waves at velocities, pressures, and gas compositions compatible with the expected flight environment [36]. The results of this testing clearly indicated that the radiation intensity measured in the experiments was inconsistent with (in fact much lower than) that predicted by the Boltzmann model, as shown in Fig. 2b. In the figure, distance is measured downstream of the normal shock in the tube, and the vertical line represents the end of the usable test time (data at larger distances from the shock are contaminated by impurities from the driver

gas). These data indicate that the Boltzmann model (red line) for Titan radiative heating is in fact incorrect for the relatively low pressures encountered during flight. A new non-local collisional-radiative model (green line) was developed based on the shock tube data [36], which is in much better agreement with the experimental data. Similar models were also developed recently at Ecole Centrale Paris [37] and EADS [38]. While more work remains to be done to fully validate these models, these results make it clear that detailed analysis and uncertainty estimation based on the Boltzmann model would be invalidated by the structural uncertainty inherent in the erroneous selection of this model to simulate the Titan radiative heating environment.

4.0 MONTE-CARLO UNCERTAINTY ANALYSIS

For systems where the uncertainties are small, a linear analysis may be used. In such an analysis, linear sensitivity coefficients are first computed. The uncertainty in the output parameter is then described by the law of propagation of errors:

$$\sigma^2(y_i) = \sum_k \left(\frac{\partial y_i}{\partial x_k} \right)^2 \sigma^2(x_k) \tag{3}$$

where $\sigma^2(y_i)$ is the variance (uncertainty) in the value of the output parameter y_i and $\sigma^2(x_k)$ is the corresponding variance in the input parameter x_k. Although computationally efficient, the linear analysis outlined here is purely local, i.e. the analysis yields sensitivity coefficients only in the neighborhood of the baseline values. However, in practice the variability in input parameters can be quite large in aerothermal and material response analysis, and the underlying models may be significantly non-linear. Therefore, a global uncertainty analysis is necessary.

Apart from the ability to handle non-linearities and large variabilities in the input and output parameters, a global model allows for the simultaneous variation of potentially large numbers of input parameters in order to account for uncertainty and sensitivity interference effects. While there are many possible statistical approaches available for the analysis of non-linear systems, we have chosen the Monte-Carlo technique, which relies on probability distribution sampling techniques to determine sensitivities and uncertainties in the numerical model under study. While Monte-Carlo analysis converges slower than some other non-linear methods (the convergence rate is proportional to the square root of the number of samples), it has the advantage that the rate of convergence is independent of the number of independent input variables considered in the model [3]. This feature makes the Monte-Carlo approach attractive for this type of aerothermal/TPS sizing analysis, where there can be literally hundreds of independent input modeling parameters in a given simulation.

In the Monte-Carlo methodology used here, the entire set of input parameters is varied independently and input/output correlation coefficients are computed via linear regression analysis. This process requires that large numbers (hundreds to thousands) of computational fluid dynamics (CFD) and material response calculations be performed in order to generate the necessary statistics with sufficient accuracy. This type of statistical analysis is commonly employed for entry trajectory design in the presence of stochastic aerodynamic, entry state, and atmospheric dispersions [39][40]. However, the methodology has only rarely been applied to TPS design [8][41], due primarily to the large cost associated with generating the number of solutions required. Fortunately, with the fairly recent advent of large, low cost parallel computing platforms and improved numerical algorithms designed specifically for their efficiency on such machines, this problem is now tractable.

4.1 Monte-Carlo Methodology

The Monte-Carlo technique outlined in this lecture can quantify and track the propagation of parametric and stochastic uncertainties that arise in a given physical model. On the other hand, structural uncertainties

cannot be quantified or even directly identified by Monte-Carlo based analysis alone; they can only be exposed via targeted ground or flight tests. In fact, a significant structural uncertainty in the model employed can completely invalidate the results of a Monte-Carlo based analysis, because the predicted trends and correlations that result will be those of the chosen model, not necessarily reality [8]. However, the analysis approach presented here can be used to design experiments that will expose structural uncertainties by displaying trends and sensitivities that are inconsistent with those predicted. The major steps in a typical Monte-Carlo uncertainty analysis are briefly summarized here. For more information see Refs. [7] & [8].

1. Parameter Identification. Input variables that need to be varied are first identified. Input variables include all modeling parameters required by the physical and numerical models employed in the simulation.

2. Initial Uncertainty Estimation. Variability limits for all input parameters are chosen that roughly represent their typical uncertainties. The variability limits need not represent the true estimated input uncertainties at this point, since they will only be used for an initial sensitivity analysis. Each input parameter is independently varied about its baseline value using an appropriate probability distribution function (typically Gaussian).

3. Sensitivity Analysis. A global sensitivity analysis is then performed by randomly varying each of the input parameters to generate CFD and/or material response simulations. It is important that sufficient runs are made for each case to ensure statistical accuracy of the resulting sensitivities. Typically hundreds to thousands of runs are required, depending on the desired accuracy of the output data.

4. Correlation Coefficient Computation. Input-output correlation coefficients are computed using linear regression analysis and the fractional contribution of each input variability to the overall output variability is obtained. For most cases the majority of the correlation is due to a small number of input parameters; the vast majority display minimal sensitivity, and thus typically warrant no further analysis. This step allows us to short list a small subset of the input parameters for a more detailed investigation.

5. Final Input Uncertainty Estimation. A more accurate estimate of the associated uncertainties for the reduced list of input parameters is then made. This can be one of the most time-consuming parts of the entire process, which is why a detailed assessment is deferred until the input uncertainties have been short listed via a sensitivity analysis. Methods of estimation for input parameter uncertainties are discussed in more detail in Refs. [7] and [26]. Unfortunately, little if any quantitative data are available for many of the parameters used in modern computational aerothermodynamics and material response models, and frequently expert judgment is the only method available.

6. Uncertainty Analysis. A second set of CFD and/or material response calculations is then made using the input uncertainties from the previous step. The function of this step is to create a database of simulation data that can be statistically analyzed.

7. Apportionment of Output Uncertainty Into Input Parameters. At the completion of Step 6, the variability in the output quantity of interest represents the true parametric uncertainty of the model to the desired level of fidelity. Finally, input-output correlations are again computed and ranked to apportion the output uncertainty into those of input parameters.

The most common approach for Step 7 (output uncertainty apportionment) is to use linear regression analysis. However, more complex approaches, which account for multi-level interference effects, can be employed if desired. Also, this step is only used in post-processing to identify the most important input

sources of final model uncertainty; the Monte-Carlo analysis method employed automatically includes all interference effects in the rolled up uncertainty value predicted.

Finally it should be noted that, although all input variables are typically assumed to vary independently, the Monte-Carlo technique as formulated does not require this. Relationships, or correlations, between input parameters can readily be modeled in the analysis if the functional forms of the relationships are known a priori. Input correlations can also be detected using principal component analysis (PCA), by which a large set of correlated input variables can be transformed into a smaller set of uncorrelated variables by means of eigenvalue analysis of their correlation matrix [42].

4.2 Example: Mars Pathfinder Convective Heating

The Mars Pathfinder aeroshell was a 2.65 meter diameter 70° sphere-cone, which entered the atmosphere of Mars on a ballistic (non-lifting) trajectory at a relative velocity of 7.5 km/s on July 4, 1997. Pre-flight calculations predicted a peak convective stagnation point heat flux of 110 W/cm^2 (Ref. [43]). As demonstrated in Ref. [26] and discussed above, the largest uncertainty for Mars laminar convective heating is the catalycity of the TPS material. A detailed uncertainty analysis of Mars Pathfinder laminar entry convective heating at the peak heating point on the trajectory was performed by Bose and Wright [26]. Since the actual catalytic properties of the surface are unknown, separate analyses were performed for each of the catalytic regimes defined by the surface reaction model discussed above and shown in Fig. 1. In addition to γ_{cat} and p_2, a total of 128 other independent parameters were varied, including chemical reaction rates, vibration-dissociation coupling parameters, vibrational relaxation times, and the binary collision integrals that make up mixture transport properties. A total of 3000 CFD runs were performed for each analysis. The nominal heating rate (Table 1) varied from 121 W/cm^2 for a supercatalytic wall to about 47 W/cm^2 for a weakly catalytic surface, a factor of 2.5 in the predicted heat flux. Uncertainty estimates on the heat flux were also determined in each catalytic regime. The largest uncertainties by far are for the moderately catalytic surface.

Table 1 Uncertainty results for the stagnation point heating of Mars Pathfinder.

Level of Catalycity	γ_{cat}	q_w (W/cm^2)	95% confidence limits (%)	
Supercatalytic	–	120.6	+10.3	-9.9
Highly catalytic	10^{-1}–10^{0}	106.7	+12.0	-17.2
Moder. catalytic	10^{-3}–10^{-1}	74.0	+41.0	-33.6
Weakly catalytic	10^{-5}–10^{-3}	47.2	+11.7	-10.6

Figure 3 shows the key input contributors to the total uncertainty as determined via linear regression analysis. It is clear that only a small number of the 130 input parameters are significant contributors to the uncertainty in heat flux. In Fig. 3 all parameters that individually contribute more than 5% to the total uncertainty are labeled with the total contribution in parentheses. The binary collision integrals, which are used to compute the species and mixture transport properties, are denoted by the two interacting species separated by a dash (–). For the limiting case of a supercatalytic wall there is no variation in the catalytic parameters (γ_{cat} and p_2) and nearly all the uncertainty in the computed heat flux comes from a small number of collision integrals that govern the rate of diffusion of the reactants to the surface. The highly catalytic wall is in the diffusion limited regime, and thus the majority of the uncertainty again comes from collision integrals, although the preference factor p_2 is also important. For the moderately catalytic wall nearly all of the uncertainty comes from γ_{cat}, indicating that we are in a rate-limited regime at these

conditions. Finally, for the weakly catalytic wall significant uncertainty arises from collision integrals which govern the thermal conductivity, as well as the rate of a single chemical reaction $O_2 + O \leftrightarrows 2O + O$, which affects heat release in the boundary layer.

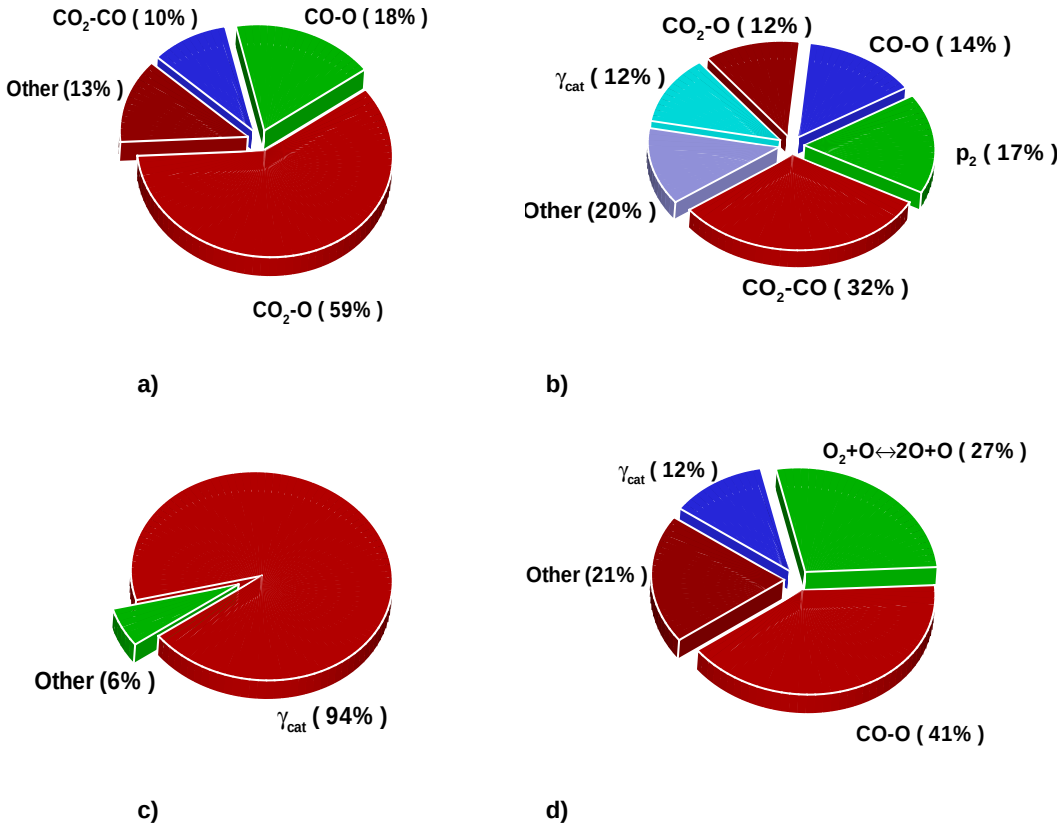

Figure 3. Principal contributors to Pathfinder heat flux uncertainty for a) super-, b) highly, c) moderately, and d) weakly catalytic wall assumption (from Ref. [26]).

From a design standpoint, it is clear that an improved understanding of surface catalysis for Mars entries could have a significant impact on TPS selection and design for future missions. One of the strengths of the technique presented here is that it can help to determine how much improvement is required. For example, if focused testing (or flight data) determined that a given material performed either as a highly catalytic or weakly catalytic surface, the current analysis indicates that further refinement in our knowledge of γ_{cat} may not be necessary, and additional research monies could be targeted to other risk drivers. However, if the material were determined to be moderately catalytic, the resulting heating uncertainties could be greatly reduced if the input uncertainty of γ_{cat} were better refined.

5.0 TPS GROUND TESTING

Although CFD and material response analysis tools have become much more sophisticated and capable in recent years, no TPS system is designed entirely with analysis. Ground testing in a relevant environment is a vital part of the TPS design process, and is used to screen materials in order to determine their suitability for a given mission, collect data to construct high-fidelity material response models, and qualify the chosen material and specific installations (penetrations, struts, tile gaps, etc.) for the flight environment. Ground testing is also used to validate the computational tools and methodologies employed in the flight

predictions, and to identify and eliminate structural uncertainties in these models. In order for the high-fidelity aeroheating and material response simulations to be used with confidence in TPS design and risk analyses, they must be verified and validated (V&V) for the specific application. Verification addresses whether the numerical models are implemented correctly [44], while validation addresses whether the simulations model the physics accurately [45]. Although the specific objectives of a given test vary considerably, the primary objectives of the overall test program should be to lower the risk profile and maximize the performance for the mission the TPS supports.

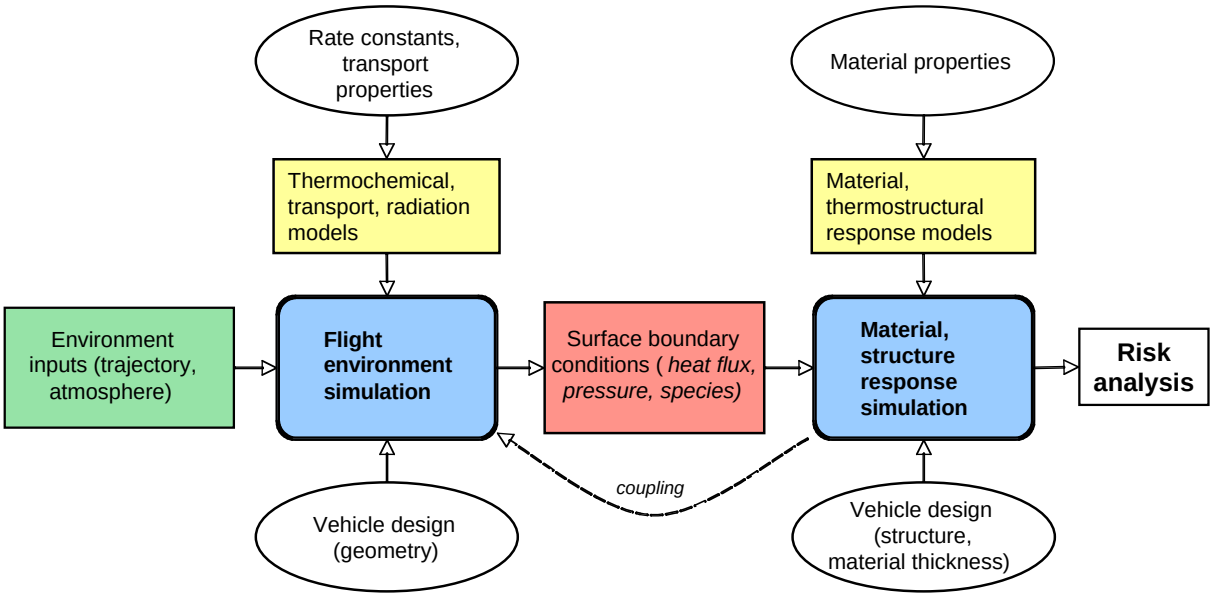

Figure 4. Elements of an analytical simulation that define the aerothermal environment and material response of a TPS. The output is used to assess performance and risk of a TPS subsystem.

The first step in developing a sound test strategy is to identify places where key validation gaps exist. A diagram indicating some (but not all) elements of an analytical simulation of TPS loads and performance is shown in Fig. 4. The analytical simulation in this context is a collection of specialized simulations supported by phenomenological models. The output is used as a performance and risk assessment metric for the TPS subsystem. TPS sizing margins and factors of safety, for example, are established based in part on the estimated uncertainties of various input parameters and test conditions. Testing should focus on reducing uncertainties that lead to the greatest risk, as determined by sensitivity and uncertainty analyses as described in Section 4. Test plans should also be constructed to maximize the chance of exposing suspected structural uncertainties in the physics models employed, and to minimize the need to extrapolate a given model from its validated range.

5.1 Facility Characteristics

High enthalpy ground testing can address uncertainties of several elements in Fig. 4. The approach depends on the features of the aerothermal, thermochemical, or thermostructural processes to be stimulated through testing. In each case, the information obtained from a test program can contribute to the validation of the overall analysis process. Improving phenomenological model accuracy, understanding failure mechanisms, or characterizing variabilities in material performance are but three examples of the ways in which analytical tools can be validated. The validation gaps and uncertainties in a particular element will define test objectives. Fulfilling those test objectives raises issues concerning the appropriate test facility, test conditions, and the test article design.

Ideally the performance of a material or system should be evaluated in a ground test simulation that closely matches the all of the significant flight environment parameters simultaneously. A well-designed ground test program would then cover the entire range of expected conditions and would fully validate the material and design for the chosen mission. However, the wide variety of length and time scales involved presents difficulties in matching relevant aerothermodynamic similarity parameters in a high enthalpy ground test simulation. Laminar stagnation point convective heat flux scales as $R^{-1/2}$ while Reynolds number scales as R, where R is the effective radius of curvature of a blunt-body test article. This limits options for matching enthalpy and more than one other similarity parameter. The nonequilibrium characteristics of high enthalpy facilities also present challenges for simulation. Time scales become important due to finite reaction and diffusion rates. Time scales impact length scales in flows with very high velocities and further complicate efforts to achieve similarity [46]. Additionally, the heat flux to a partially catalytic surface is sensitive to the thermodynamic state at the boundary layer edge which, in turn, can depend on the degree of thermochemical nonequilibrium in the freestream [47]. More importantly, some mission-specific aspects can be simulated only partially or not at all [11]. For example, time-varying conditions of an entry profile cannot be achieved in most facilities. Arc plasma facilities that can accommodate non-terrestrial gas mixtures (e.g. CO_2/N_2 for Mars and Venus) at relevant enthalpies and test article sizes may not be available. The capability to simulate combined radiative-convective heating environments, such as would be encountered during a crewed lunar or Mars return entry, no longer exists in the United States.

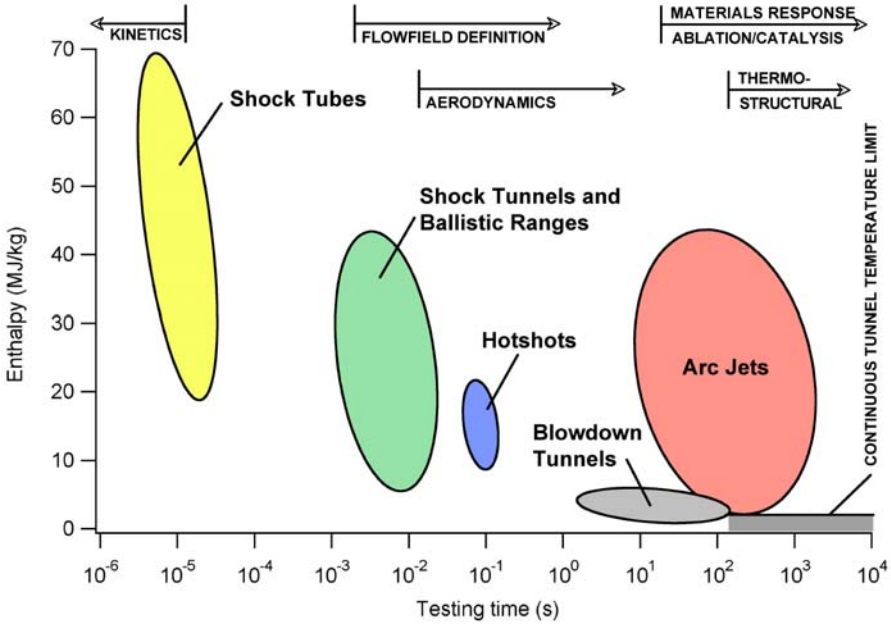

Figure 5. High enthalpy test facility capabilities and applications.

Figure 5 shows the types of facilities and the elements of TPS development they are capable of simulating. Both the enthalpy range and the testing time influence their role in validation strategies. With their short testing times, impulse facilities (e.g. shock tubes, shock tunnels, and ballistic ranges) are suitable primarily for studying aeroheating as well as gas-kinetic and radiation processes. Material response mechanisms have much slower timescales and can only be evaluated in facilities that operate for long durations. Although several types of long-duration facilities, such as radiative lamps, lasers, and combustion-driven flows, are routinely used to achieve specific test objectives, arc jets have been the workhorse facilities for the past 40 years to support material response model development and subsystem-scale hardware performance validation. Arc jets provide the means for TPS materials to reach flight temperatures under conditions where surface chemistry effects approximate that of flight. Large-scale, low-pressure arc jet

facilities in particular accommodate near flight-scale test articles, permitting simulations at appropriate enthalpies and laminar Reynolds numbers. For this reason they are the primary test facilities that are used to flight-qualify TPS materials for civilian entry vehicles within NASA. A survey of large-scale arc-heated facilities worldwide can be found in Ref. [48].

5.2 Arc Jet Testing Methodology

In an arc jet, a series of electrodes are used to arc heat the gas prior to expansion. This heated gas is then passed through a nozzle to expand the flow to reach temperatures and pressures of interest to flight. Arc heating of the gas stream produces a significant amount of dissociation and ionization. In the plenum region prior to the nozzle expansion, the gas is in thermo-chemical equilibrium at temperatures on the order of 7000 K. During the expansion through the nozzle, the flow accelerates rapidly and the stream is left in a state of thermo-chemical nonequilibrium as various kinetic process freeze at different times due to the differing timescales of thermal and chemical relaxation in the flow. For air flows, a significant portion of the total flow enthalpy remains in dissociated N_2 and O_2; the flow is chemically frozen at temperatures for which much less dissociation would exist in chemical equilibrium. This increase in chemical enthalpy reduces the velocity of the stream – energy locked in chemical nonequilibrium is unavailable as kinetic energy. The dissociated free stream reduces the Mach number due to both a lower velocity and higher sound speed. This affects the shock standoff distance observed in the test. Dissociation also increases the density over what would result at equilibrium for the same total enthalpy. The composition at the boundary layer edge is also affected, altering the amount of chemical energy available for surface recombination. Therefore, matching total enthalpy and surface pressure in flight and arc jet environments does not necessarily yield the same heat flux to a partially catalytic material [47]. This potential difference in heat flux underscores one of the principal challenges in establishing ground-to-flight traceability.

In all cases, the confidence in any causal relationship between test conditions and test observables rests upon the accuracy to which the test conditions are known. The selection of appropriate conditions for a given test requires detailed knowledge of a facility's operating characteristics, with enthalpy and pressure being most important among the relevant parameters. Pressure is typically determined with pitot probe surveys of the test section. Unfortunately, enthalpy can be particularly difficult to measure in an arc jet, and significant discrepancies are frequently observed between different intrusive and non intrusive measurement techniques. In complement to experimental techniques, high fidelity simulation techniques for arc jet flows can provide unique insight into a particular facility's nonequilibrium thermochemistry; this type of information is typically unavailable via conventional flow diagnostics. Considerable attention has been devoted in recent years to understanding the operating characteristics of arc jet facilities [49][50]. Applied to the test planning process, arc jet flow simulation is a tool that can be employed to rapidly explore potential test configurations and optimize the return on investment in testing resources to meet program objectives. The merits of a particular test design can be identified and understood early in the planning process. Most importantly, by using the same CFD flow solver for both arc jet and flight environment simulation, consistency between flight environment definition and test interpretation can be maintained – a critical need in resolving ground-to-flight traceability.

An end-to-end simulation of an arc jet test involves 1) a nozzle calculation that defines the arc jet free stream conditions, 2) a model calculation of the flow over the test article, and 3) a transient thermo-structural analysis of the test article including material thermal response. Facility data (such as flow rates) and test observables (such as pressure, heat flux, model temperatures, and emissivity) are incorporated as boundary conditions. An example of a virtual arc jet simulation is depicted in Fig. 6. The simulation is of a typical candidate TPS material "flat-face" coupon tested in a stagnation configuration. The overall test simulation procedure is as follows. First, stream conditions are determined via a CFD simulation of the nozzle flow, based on prescribed (from facility data) conditions at the nozzle throat. A second CFD calculation is then performed of the flow over the test article with prescribed surface boundary conditions, using freestream conditions extracted from the nozzle simulation. Environment parameters that cannot at

present be measured (or are not measured routinely) such as shear stress, Reynolds number, or species mass fractions, can then be extracted directly from solutions. The surface temperature time history is typically a primary metric by which the performance of a TPS material is assessed. However, the surface temperature is controlled in large part by the efficiency with which the incident heat flux is dissipated by other loss mechanisms at the surface: re-radiation, conduction, and, in the case of ablators, surface reactions, pyrolysis, and mass transfer. Also, the thermal properties of the test article and the model holder also can have a large effect on the results. Therefore, thermal analysis of arc jet model designs is a crucial part of any test planning process to ensure that relevant thermal losses are incorporated.

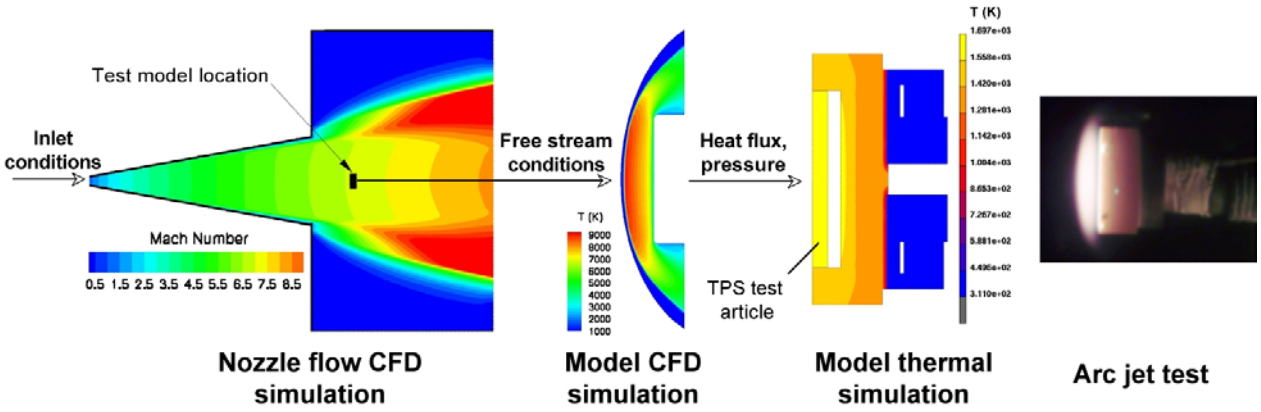

Figure 6. Virtual arc jet simulation. Facility operating parameters are inlet conditions for the CFD nozzle calculation. Nonequilibrium free stream conditions from the nozzle solution become the upstream boundary condition for the CFD solution of the test model. The thermal response of the model is then computed with a finite element simulation using boundary conditions from the model solution.

Without validation of the arc jet CFD simulations, test observations may not be accurately – or correctly – captured in the material response models. Detailed chemical and physical measurements of arc jet flow properties and their spatial distribution could help reduce uncertainties in the simulations. Accounting for all contributions to the enthalpy at a particular point requires several measurements, with the minimum being velocity, temperature, and species densities. One of the more useful tools for performing nonintrusive optical measurements in arc jet flows is laser-induced fluorescence (LIF), a spatially resolved, species-selective probe of individual atomic and molecular states. LIF of atomic nitrogen has been applied to directly measure the velocity, translational temperature, and nitrogen number density in the free stream of arc jet facilities [51][52]. The kinetic, thermal, and chemical modes of the total enthalpy can be quantified with the LIF data and other facility measurements [51]. Optical diagnostics have also been developed for the shock layer region ahead of blunt body test articles. Emission spectra have been analyzed in an effort to characterize flow properties within the shock layer and their relation to the free stream. Spectra at multiple points along the stagnation streamline were compared to those from simulations to assess the degree of chemical or thermal nonequilibrium within the shock layer [53]. Time resolved emission spectra and optical attenuation ahead of an ablating test model have been recorded with novel fiber optic- and laser-based instruments [54]. Other advanced non-intrusive techniques are also under development, including methodologies for measuring time-dependent recession during testing. These diagnostics provide insight on the transient performance of ablative TPS materials that can support the development of improved gas-surface interaction and in-depth thermal response models.

5.3 Example: Mars Exploration Rover TIRS Cover Testing

The twin Mars Exploration Rover (MER) entry vehicles successfully landed on Mars in January 2004. The MER aeroshell was initially intended to replicate that of Mars Pathfinder. However, one significant change was the addition of three Transverse Impulse Rocket System (TIRS) motors on the backshell,

intended to minimize lateral velocity while on parachute and at ground impact. Because these TIRS motors (of necessity) protruded through the backshell, TPS covers were required to protect the motors from the entry environment. These covers were designed to be jettisoned before the TIRS became active on terminal descent. The design of the protective cover and its interface with the backshell was validated through arc jet testing in the 20 Megawatt Panel Test Facility (PTF) at NASA Ames Research Center [55]. Heating environment predictions from flight CFD solutions including the TIRS covers defined the heat flux, heat load, and pressure on the cover and at the interface seal. The maximum local heat flux to the cover occurs on the aft end due to the large recirculation region on the backshell. Final sizing for the TIRS cover TPS was based on these analyses and included margins due to uncertainties arising from transition to turbulence and aerothermal environment variations.

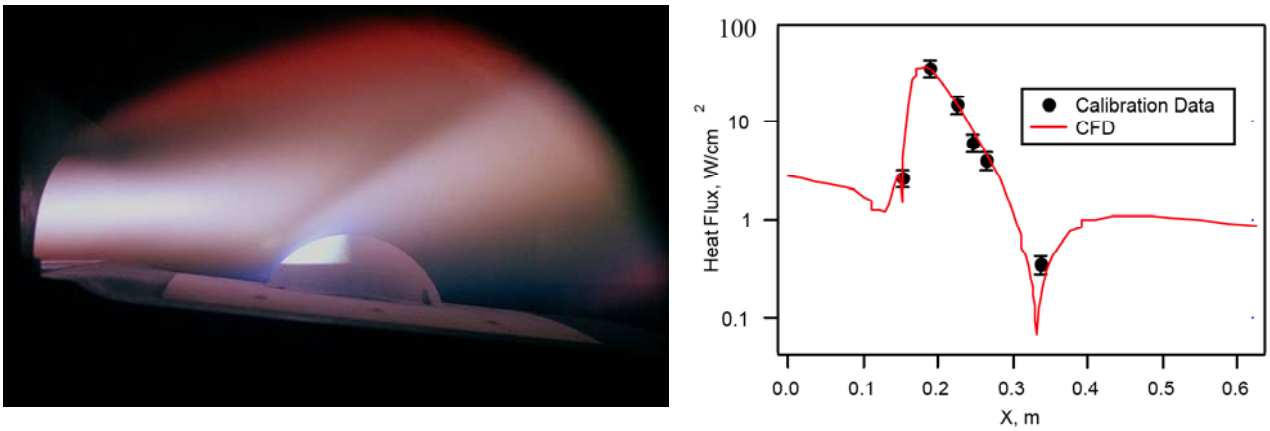

a) b)

Figure 7. a) TIRS cover calibration model in the PTF arc jet. b) Comparison of measured and simulated heat flux along the TIRS cover centerline for the calibration test. The origin (X = 0) begins at the nozzle exit.

Design validation of the TIRS cover seal at its interface with the backshell was a primary test objective. A full-scale flight article was tested at flight-representative heat fluxes and pressures along the gap between the cover and simulated backshell. A pressure differential across the seal was maintained, and the test model design incorporated a witness plate below the cover attachment as a means to monitor seal performance. The large, recirculating flow that heats the aft end of the cover could not be reproduced with relevant similarity in an arc jet test. Instead, turning the cover to face the stream approximated the predicted heating distribution. However, because of the differing complex 3-D flow features of both the arc jet and flight environment, the heat flux and pressure distributions on the cover did not compare favorably at all locations. This test case illustrates the difficulty in maintaining ground-to-flight traceability when it is impossible to simultaneously reproduce all aspects of the flight environment. In this case, the primary objective was to evaluate the thermostructural performance of the seal, and thus necessary compromises were made in other areas. CFD simulations of the nozzle flow with the TIRS cover test article were used to determine the test conditions (facility flow rate, enthalpy, and test panel inclination) that best matched the predicted peak heat load and surface pressure along the gap region. A calibration test article instrumented with calorimeters and thermocouples was used to validate these pre-test analyses. The calibration model under test is shown in Fig. 7a. Centerline heat flux measurements compare favorably with the CFD solution (Fig. 7b). Subsequent tests at the calibrated test condition were used to assess the performance of the TIRS cover seal. The connection between the test and flight conditions for the heat flux and pressure along the seal was defined through the CFD simulations. The calibration test confirmed the pre-test prediction and demonstrated that CFD can be used successfully as a test planning tool.

5.4 Example: Wing Leading Edge Testing

A test series was recently performed in the 60 Megawatt Interaction Heating Facility (IHF) at NASA Ames to evaluate the performance of a candidate RLV wing leading edge TPS design. Because of the complex nature of this test series, three-dimensional arc jet CFD simulations were essential to establish appropriate conditions and test article design for a representative arc jet test that would best simulate a wing leading edge flight environment [56]. The primary objective of the test was to evaluate the thermostructural performance of a candidate leading edge TPS assembly, including attachments, gaps and seams. The IHF arc jet, when equipped with a semi-elliptic nozzle, provides a boundary layer flow appropriate for reaching high Reynolds numbers with boundary layer edge characteristics comparable to flight. A swept pylon test model was designed to simulate the flow along the curved leading edge and its intersection with the incoming boundary layer. The arc jet operating parameters and final model dimensions were chosen through the pre-test CFD analysis to match the flight predictions of heat flux, boundary layer edge Mach number, boundary layer thickness, and Reynolds number as closely as possible. Figure 8 is a photograph of the pylon leading edge model during an IHF arc jet test. The thickness of the incoming boundary layer and the leading edge shock location can be inferred visually from the change in emission intensity of the stream.

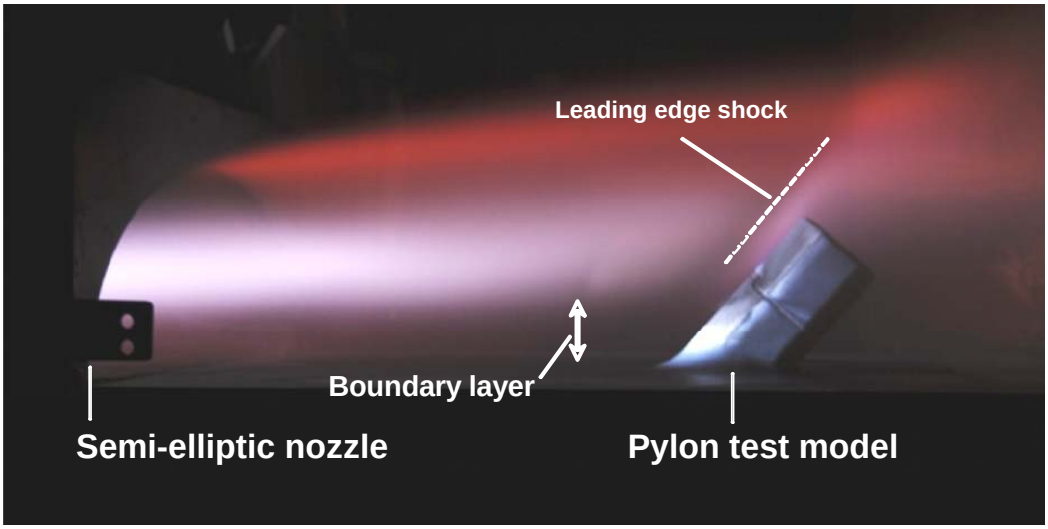

Figure 8. Arc jet test of a test model used to simulate wing leading edge heating. The boundary layer thickness and leading edge shock location can be discerned by the change in the emission intensity of the free stream.

The simulation and test results were used in a finite-element analysis to assess the thermostructural response of a candidate leading edge system. The test model included features of a leading edge assembly that required performance validation. The heat flux and pressure distributions from the CFD solution were applied as boundary conditions for the finite element simulation. The CFD simulation was necessary to optimize the test design and facility operating conditions, confirm measured material surface temperatures, and define the boundary condition distributions for the finite element analysis.

6.0 FLIGHT TESTING

Although most TPS systems are designed exclusively with analysis and ground testing, flight testing remains the only way to fully validate the performance of a full-scale thermal protection system in a new environment. In addition, certain structural uncertainties in the aeroheating or material response model can only be exposed through flight testing. Unfortunately, the prohibitively high cost of full-scale flight testing

implies that such tests, if carried out at all, must be carefully designed and executed. Such testing should if possible be reserved for final model and system-level validation, once we have good physics-based models of the expected environment and resulting material performance based on ground-test and historical data. However, valuable information on TPS flight performance can frequently be obtained via much less expensive sub-scale tests, as long as these tests are well designed to ensure that they reasonably simulate the full-scale flight environment.

6.1 Example: Apollo Flight Test Program

An excellent example of a well designed flight test program was that carried out in support of Apollo; the primary test objectives relating to aerothermal analysis and TPS validation are briefly reviewed here. The Apollo Command Module was the first human-rated lunar return entry vehicle, and it was also the first spacecraft that employed a mid-density ablator (Avcoat) for primary thermal protection. As such, an extensive series of flight tests were planned to obtain data for model development and to validate the performance of a new TPS material for such an environment. A total of six large scale flight tests were flown. The first two, called Project Fire, had a primary objective to collect data on shock layer radiative heating at lunar return velocities [57]. The motivation for this program was the large disparity in radiative heating design predictions for the Apollo return capsule. Several models for shock heating were employed during the Apollo design phase, and predictions of the total heating rate from shock layer radiation varied by more than a factor of three, [58] indicating the presence of a possibly large structural uncertainty in one or all of the models. While some validation data were obtained in ground-test facilities (primarily shock tubes), these data were not considered sufficient to resolve this issue to the level of confidence required for a human-rated system. Unfortunately, flight data from the Fire-I flight were compromised by a stage separation problem [59], but radiative heating measurements from Fire-II were generally in good agreement with the lower bound of pre-flight predictions. These data have since been used for validation and calibration of a variety of nonequilibrium air radiation models [60].

During the development phase of the low-density Avcoat TPS material, ground tests were conducted in almost every arc jet facility in the United States. However, attempts to correlate these data into a single material response model were frustrating, because the results from different facilities indicated vastly different characteristics, ranging from catastrophic failure to excellent performance [61]. Early sub-scale flight experiments showed similar variability in material performance. One notable example was the R-4 flight test [62], in which the measured ablation rate was much higher than predicted; in fact, the entire ablative nosecap was eroded away during the entry. The root cause of the catastrophic failures observed during ground and flight testing was eventually determined to be the extremely high dynamic pressures of these tests. For example, the R-4 flight test was conducted at dynamic pressures three times that expected during Apollo entry, in an attempt to increase the heat transfer rate. Although the root cause of the problems was eventually determined, a great deal of effort was expended to prove this fact to the satisfaction of all involved. One of the primary lessons learned from this experience was that ground or flight testing in non-representative environments can be highly misleading and cause unwarranted concern [62]. In other words, a poorly conceived test can be far worse than no test at all.

In part because of the concerns raised during ground testing of the TPS, a series of four flight tests of the full scale Apollo Command Module were flown: two at orbital velocity [63], and two at superorbital velocity representative of lunar return [64]. Some of the primary objectives of the flight tests were to obtain aeroheating and TPS material response data to validate the analytical design tools and the overall performance of the ablator system. Each of these capsules was heavily instrumented with calorimeters (surface and in-depth), char sensors, pressure transducers, and shock-layer radiometers [62]. In addition, the heatshields were recovered and core samples of the post-flight TPS material were analyzed extensively [65][66]. The results of this analysis and flight data reduction indicated that the material performed extremely well under lunar entry conditions. In fact, measured performance was much better than pre-flight predictions. Among other things, the total TPS material recession more than an order of magnitude

less than even the most conservative predictions. The reasons for this discrepancy were eventually traced to a significant structural uncertainty in the existing material response models (none accounted for the char coking phenomenon [61]). Once the models were updated to account for this effect, the agreement with flight data was excellent [66].

Finally, it is important to note that there are other ways to obtain useful flight data other than full-scale tests. Sub-scale testing, via sounding rockets or similar launch platforms, can provide valuable data for component design and analysis for a (relatively) small cost. Placing instrumentation on the heatshield of science (e.g. Mars Pathfinder [25]) and human exploration (e.g. Shuttle Orbiter [67]) missions once was standard engineering practice. These data provide valuable model validation information at a relatively low per-mission cost. Unfortunately, recent practice has been to eliminate such instrumentation as a cost savings measure. For example, neither the ESA Huygens probe nor the NASA MER rovers carried any active instrumentation on the heatshield. Each mission would have provided a prime opportunity to investigate key modeling gaps for future Titan and Mars entries, respectively, as discussed in previous sections. The decision to eliminate instrumentation on recent missions was primarily motivated by cost-savings. This decision is somewhat understandable given that, in general, a given mission does not benefit directly from the engineering instrumentation that it carries. Therefore, from the standpoint of the mission manager, inclusion of heatshield instrumentation adds cost, complexity and risk to the entry without a corresponding mission benefit. The benefits become apparent only when looked at from the viewpoint of an overall exploration program, for which the engineering data from each individual mission are laying the groundwork for the presumably more complex missions to follow.

7.0 SUMMARY AND CONCLUSIONS

A methodology was presented for the risk based design and analysis of thermal protection systems for Earth and planetary entry vehicles. The first step in the process is the identification of key modeling deficiencies via a mission-specific gap analysis. Once these modeling deficiencies are identified, Monte-Carlo based sensitivity and uncertainty analyses are conducted to quantify parametric and stochastic uncertainties in the models employed. It is important to note that structural uncertainties, or basic deficiencies in the models employed for simulation, cannot be identified by this approach alone. However, the results of a sensitivity analysis can be used to design tests to expose these structural uncertainties by quantifying trends that should be reproducible by a well designed test series. These techniques also facilitate a risk-based probabilistic design approach, whereby the TPS can be designed to a desired risk tolerance level, and remaining risk can be effectively compared to and traded with that of other subsystems via a system level risk mitigation analysis. Modeling sensitivities, which are a by-product of the uncertainty analysis, can be used to rank input uncertainty drivers, which can then be prioritized and targeted for further analysis or testing. Examples of structural uncertainty identification and parametric uncertainty quantification are given for Mars and Titan entry problems. These examples demonstrate the utility of the methodology to quantify the uncertainty levels, rank sources of input uncertainty, identify structural uncertainties in the models employed, and probabilistically design a TPS system for a planetary entry mission.

Although high-fidelity analysis is used increasingly earlier in the design cycle as the tools and methods become faster and more accurate, ground-based testing remains a critical component of the design of any TPS system. Given that it is seldom possible to simultaneously match all aspects of the flight environment in any ground test facility, great care must be taken in the design of any test series to ensure traceability to the flight environment. The various types of ground test facility commonly employed in TPS design are discussed briefly, but the paper focuses on arc jets, which have been the primary TPS testing workhorse facility for the past 40 years. This paper outlines a testing methodology designed to ensure that the tests performed are flight-relevant and focused on driving down key risks and/or uncertainties in the flight design. This methodology is based on experimental diagnostics (both intrusive and non-intrusive),

augmented by high-fidelity simulations of the arc jet test environment. Examples are given for the design of flight hardware on the Mars Exploration Rovers, and the preliminary design of an RLV wing leading edge concept. Finally, the role of flight testing in TPS design is discussed. The high cost of full-scale flight testing generally limits its role to one of final model validation in a new flight environment. Examples are given from the Apollo program highlighting both the benefits of a well constructed flight test program, and the dangers of poorly conceived flight experiments.

ACKNOWLEDGEMENTS

The authors would like to thank Y.-K. Chen (NASA Ames), Peter Gage (ELORET), Tahir Gökçen (ELORET), Dean Kontinos (Ames), Bernard Laub (Ames), Ryan McDaniel (Ames), Grant Palmer (ELORET), Dave Stewart (Ames), and Michael Wilder (Ames) for manuscript suggestions and improvements. Technical discussions with Joe Marschall (SRI) were extremely helpful in understanding Mars surface catalysis models. Finally, the authors thank Michelle Munk (NASA Marshall) and Bonnie James (Marshall) of the NASA In-Space Propulsion Program for their unwavering support of the Monte-Carlo uncertainty analysis work.

REFERENCES

[1] Hall, J.L., Noca, M.A., and Bailey, R.W., "Cost-Benefit Analysis of the Aerocapture Mission Set," *Journal of Spacecraft and Rockets*, Vol. 42, No. 2, 2005, pp. 309-320.

[2] Thacker, B., Riha, D., Millwater, H., and Enright, M., "Errors and Uncertainties in Probabilistic Engineering Analysis," AIAA Paper No. 2001-1239, Jan. 2001.

[3] Garzon, V. and Darmofal, D., "Using Computational Fluid Dynamics in Probabilistic Engineering Design," AIAA Paper No. 2001-2526, Jun. 2001.

[4] Gnoffo, P.A., Weilmuenster, K.J., Hamilton, H.H., Olynick, D.R., and Venkatapathy, E.V., "Computational Aerothermodynamic Design Issues for Hypersonic Vehicles," *Journal of Spacecraft and Rockets*, Vol. 36, No. 1, 1999, pp. 21-43.

[5] Avco Corporation, "Ablation Handbook, Entry Materials Data and Design," Technical Report AFML-TR-66-262, Sep. 1966.

[6] Coleman, W.D., Hearne, L.F., Lefferdo, J.M., Gallagher, L.W., and Vojvodich, N.S., "Effects of Environmental and Ablator Performance Uncertainties on Heat-Shielding Requirements for Hyperbolic Entry Vehicles," *Journal of Spacecraft and Rockets*, Vol. 5, No. 11, 1968, pp. 1260-1270.

[7] Bose, D., Wright, M.J., and Gökçen, T., "Uncertainty and Sensitivity Analysis of Thermochemical Modeling for Titan Atmospheric Entry," AIAA Paper No. 2004-2455, Jun. 2004.

[8] Wright, M.J., Bose, D., and Chen, Y.-K., "Probabilistic Modeling of Aerothermal and Material Response Uncertainties for Aerocapture Using Rigid Aeroshells," 53rd JANNAF Joint Propulsion Meeting, Dec. 2005.

[9] Park, C., "Laboratory Simulation of Aerothermodynamic Phenomena: A Review," AIAA Paper No. 92-4025, Jul. 1992.

[10] Grinstead, J., Stewart, D., and Smith, C., "High Enthalpy Test Methodologies for Thermal Protection Systems Development at NASA Ames Research Center," AIAA Paper No. 2005-3326, May 2005.

[11] Laub, B., Balboni, J., and Goldstein, H., "Ground Test Facilities for TPS Development," NASA TM-2002-211400, May 2002.

[12] Palmer, G.E., Kontinos, D.A., and Sherman, B., "Surface Heating Effects of X-33 Vehicle TPS Panel Bowing, Steps, and Gaps," AIAA Paper No. 98-0865, Jan. 1998.

[13] Reuther, J., Prabhu, D., Brown, J., Wright, M., and Saunders, D., "Computational Fluid Dynamics for Winged Reentry Vehicles at Hypersonic Conditions," AIAA Paper No. 2004-2537, Jun. 2004.

[14] Richardson, E., Munk, M., and James, B., "Review of NASA In-Space Propulsion Technology Program Inflatable Decelerator Investments," AIAA Paper No. 2005-1603, May 2005.

[15] Gulick, D., Lewis, J., Trochman, B., Stein, J., Lyons, D., and Wilmoth, R., "Trailing Ballute Aerocapture: Concept and Feasibility Assessment," AIAA Paper No. 2003-4655, Jul. 2003.

[16] Papadopoulos, P., Prabhu, D., Olynick, D., Chen, Y.-K., and Cheatwood, F.M., "CFD Code Comparisons for Mars Entry Simulations," AIAA Paper No. 98-0272, Jan. 1998.

[17] Edquist, K., Liechty, D., Hollis, B., Alter, S., and Loomis, M., "Aeroheating Environments for a Mars Smart Lander," AIAA Paper No. 2002-4505, Aug. 2002.

[18] Mitcheltree, R.A., and Gnoffo, P.A., "Wake Flow about the Mars Pathfinder Entry Vehicle," *Journal of Spacecraft and Rockets*, Vol. 32, No. 5, 1995, pp. 771-776.

[19] Christmann K., Introduction to Surface Physical Chemistry, Springer-Verlag, New York, 1991.

[20] Kolesnikov, A., Yakushin, M., Pershin, I., and Vasil'evskii, S., "Heat Transfer Simulation and Surface Catalycity Prediction at the Martian Atmosphere Entry Conditions," AIAA Paper 99-4892, Aug. 1999.

[21] Sepka, S., Chen, Y.-K., Marschall, J., and Copeland, R., "Experimental Investigation of Surface Reactions in Carbon Monoxide and Oxygen Mixtures," *Journal of Thermophysics and Heat Transfer*, Vol. 14, No. 1, 2000, pp. 45-52.

[22] Afonina, N.E., Gromov, V.G., and Kovalev, V.L., "Catalysis Modeling for Thermal Protection Systems of Vehicles Entering into Martian Atmosphere," AIAA Paper No. 2001-2832, Jun. 2001.

[23] Rini, P., Garcia, A., Magin, T., and Degrez, G., "Numerical Simulation of CO_2 Nonequilibrium Flows with Catalyzed Surface Reactions," AIAA Paper No. 2003-4038, Jun. 2003.

[24] Marschall, J., Copeland, R.A., Hwang, H.H., and Wright, M.J., "Surface Catalysis Experiments on Metal Surfaces in Oxygen and Carbon Monoxide Mixtures," AIAA Paper No. 2006-0181, Jan. 2006.

[25] Milos, F.S., Chen, Y.-K., Congdon, W.M., and Thornton, J.M., "Mars Pathfinder Entry Temperature Data, Aerothermal Heating, and Heatshield Material Response," *Journal of Spacecraft and Rockets*, Vol. 36, No. 3, 1999, pp. 380-391.

[26] Bose, D. and Wright, M.J., "Uncertainty Analysis of Laminar Aeroheating Predictions for Mars Entries," AIAA Paper No. 2005-4682, Jun. 2005.

[27] Wright, M., Olejniczak, J., Walpot, L., Raynaud, E., Magin, T., Caillaut, L., and Hollis, B., "A Code Calibration Study for Huygens Entry Aeroheating," AIAA Paper No. 2006-0382, Jan. 2006.

[28] Hollis, B., Horvath, T., Berry, S., Hamilton, H., and Alter, S., "X33 Computational Aeroheating Predictions and Comparisons with Experimental Data," AIAA Paper No. 99-3559, Jun. 1999.

[29] Gnoffo, P.A., "CFD Validation Studies for Hypersonic Flow Predictions," AIAA Paper No. 2001-1025, Jan. 2001.

[30] Wright, M.J., Loomis, M.A., and Papadopoulos, P.E., "Aerothermal Analysis of the Project Fire II Afterbody Flow," *Journal of Thermophysics and Heat Transfer*, Vol. 17, No. 2, 2003, pp. 240-249.

[31] Wright, M.J., Prabhu, D.P., and Martinez, E.R., "Analysis of Apollo Command Module Afterbody Heating, Part 1: AS-202," AIAA Paper No. 2004-2456, Jun. 2004.

[32] Baillion, M., Taquin, G., and Soler, J., "Huygens Radiative Probe Environment," *Proceedings of the 19th International Symposium on Shock Waves*, 1993, pp. 339-346.

[33] Baillion, M. and Taquin, G., "Radiative Heat Flux: Theoretical and Experimental Predictions for Titan Entry Probe," *Capsule Aerothermodynamics*, AGARD Report No. 808, pp. 9/1-9/30, May 1997.

[34] Olejniczak, J., Wright, M., Prabhu, D., Takashima, N., Hollis, B., Zoby, E., and Sutton, K., "An Analysis of the Radiative Heating Environment for Aerocapture at Titan," AIAA Paper No. 2003-4953, Jul. 2003.

[35] Wright, M.J., Bose, D., and Olejniczak, J., "The Impact of Flowfield-Radiation Coupling on Aeroheating for Titan Aerocapture," *Journal of Thermophysics and Heat Transfer*, Vol. 19, No. 1, 2005, pp. 17-27.

[36] Bose, D., Wright, M.J., Raiche, G., Bogdanoff, D., and Allen, G.A., "Modeling and Experimental Validation of CN Radiation Behind a Strong Shock Wave," AIAA Paper No. 2005-0768, Jan. 2005.

[37] Magin, T.E., Caillaut, L., Bourdon, A., and Laux, C.O., "Nonequilibrium Radiation Modeling for Huygens Entry," *Proceedings of the 3rd International Planetary Probe Workshop*, Jul. 2005.

[38] Raynaud, E., Tran, P., Soler, J., and Baillion, M., "Huygens Aerothermal Environment: Radiative Heating," *Proceedings of the 3rd International Planetary Probe Workshop*, Jul. 2005.

[39] Spencer, D. and Braun, R., "Mars Pathfinder Atmospheric Entry: Trajectory Design and Dispersion Analysis," *Journal of Spacecraft and Rockets*, Vol. 33, No. 5, 1996, pp. 670-676.

[40] Desai, P. and Cheatwood, F.M., "Entry Dispersion Analysis for the Genesis Sample Return Capsule," *Journal of Spacecraft and Rockets*, Vol. 38, No. 3, 2001, pp. 345-350.

[41] Dec, J.A. and Mitcheltree, R.A., "Probabilistic Design of Mars Sample Return Earth Entry Vehicle Thermal Protection System," AIAA Paper No. 2002-0910, Jan. 2002.

[42] Kachigan, S.K., Multivariate Statistical Analysis: A Conceptual Introduction, Radius Press, New York, NY, 1982.

[43] Chen, Y.-K., Henline, W.D., and Tauber, M.E., "Mars Pathfinder Trajectory Based Heating and Ablation Calculations," *Journal of Spacecraft and Rockets*, Vol. 32, No. 2, 1995, pp. 225-230.

[44] Roy, C., Oberkampf, W., and McWherter-Payne, M., "Verification and Validation for Laminar Hypersonic Flowfields, Part 1: Verification," *AIAA Journal*, Vol. 41, No. 10, 2003, pp. 1934-1943.

[45] Roy, C., Oberkampf, W., and McWherter-Payne, M., "Verification and Validation for Laminar Hypersonic Flowfields, Part 2: Validation," *AIAA Journal*, Vol. 41, No. 10, 2003, pp. 1944-1954.

[46] Inger, G.R., "Scaling Nonequilibrium-Reacting Flows: The Legacy of Gerhard Damköhler," *Journal of Spacecraft and Rockets*, Vol. 38, No. 2, 2001, pp. 185-190.

[47] Gökçen, T., "Effects of Flowfield Nonequilibrium on Convective Heat Transfer to a Blunt Body," *Journal of Thermophysics and Heat Transfer*, Vol. 10, No. 2, 1996, pp. 234-241.

[48] Smith, R.K., Wagner, D.A., and Cunningham, J. "A Survey of Current and Future Plasma Arc-Heated Test Facilities for Aerospace and Commercial Applications," AIAA Paper No. 98-0146, Jan. 1998.

[49] Loomis, M., Hui, F., Polsky, S., Venkatapathy, E., and Prabhu, D., "Arc-Jet Semi-Elliptic Nozzle Simulations and Validation in Support of X-33 TPS Testing," AIAA Paper No. 98-0864, Jan. 1998.

[50] Olejniczak, J. and Fletcher, D.G., "An Experimental and Computational Study of the Freestream Conditions in an Arc-Jet Facility," AIAA Paper No. 2000-2567, Jun. 2000.

[51] Fletcher, D.G., "Arcjet Flow Properties Determined From Laser-Induced Fluorescence of Atomic Nitrogen," *Applied Optics*, Vol. 38, No. 9, 1999, pp. 1850-1858.

[52] Grinstead, J., Driver, D., and Raiche, G., "Radial Profiles of Arcjet Flow Properties Measured with Laser-Induced Fluorescence of Atomic Nitrogen," AIAA Paper No. 2003-0400, Jan. 2003.

[53] Fletcher, D.G., Raiche, G.A., and Prabhu, D.K., "A Method for Determining Species Mass Fractions From Spectrally Resolved Emission Measurements," AIAA Paper No. 2000-2699, Jun. 2000.

[54] Raiche, G. and Driver, D., "Shock Layer Optical Attenuation and Emission Spectroscopy Measurements During Arc Jet Testing with Ablating Models," AIAA Paper No. 2004-0825, Jan. 2004.

[55] Szalai, C., Chen, Y.-K., Loomis, M., Thoma, B., and Buck, S., "Mars Exploration Rover Transverse Impulse Rocket Cover Thermal Protection System Design Verification," *Journal of Spacecraft and Rockets*, Vol. 42, No. 6, 2005, pp. 990-998.

[56] Gökçen T. and Stewart, D., "Computational Analysis of Semi-elliptical Nozzle Arc-jet Experiments," AIAA Paper No. 2005-4887, Jun. 2005.

[57] Cauchon, D.L., "Radiative Heating Results from the Fire II Flight Experiment at Reentry Velocity of 11.4 km/s," NASA TM X-1402, Jul. 1967.

[58] Anderson, J.D., "An Engineering Survey of Radiating Shock Layers," AIAA Paper 68-1151, Dec. 1968.

[59] Woodbury, G., "Angle of Attack Analysis for Project Fire I Reentry Flight," NASA TN D-3366, 1966.

[60] Olynick, D., Henline, W., Hartung-Chambers, L., and Candler, G., "Comparison of Coupled Radiative Flow Solutions with Project Fire II Flight Data," *Journal of Thermophysics and Heat Transfer*, Vol. 9, No. 4, 1995, pp. 586-594.

[61] Laub, B., "The Apollo Heatshield: Why Performance Exceeded Expectations," *Proceedings of the International Symposium on Atmospheric Reentry Vehicles and Systems*, Arcachon, France, Mar. 1999.

[62] Pavlosky, J.E. and St. Leger, L.G., "Apollo Experience Report: Thermal Protection Subsystem," NASA TN D-7564, Jan. 1974.

[63] Lee, D., Bertin, J., and Goodrich, W., "Heat Transfer Rate and Pressure Measurements During Apollo Orbital Entries," NASA TN D-6028, Oct. 1970.

[64] Lee, D. and Goodrich, W., "Aerothermodynamic Environment of the Apollo Command Module During Superorbital Entry," NASA TN D-6792, Apr. 1972.

[65] Bartlett, E.P., "Improved Heat Shield Design Procedures for Manned Entry Systems, Part II: Application to Apollo," NASA CR108689, Jun. 1970.

[66] Bartlett, E.P., "An Evaluation of Flight Data for the Apollo Thermal Protection System," *Space Simulation*, pp. 749-768, Jan. 1972.

[67] Thompson, R., "Comparison of Nonequilibrium Viscous-Shock-Layer Solutions With Shuttle Heating Measurement," *Journal of Thermophysics and Heat Transfer*, Vol. 4, No. 2, 1990, pp. 162-169.